ELSEVIER

Tectonophysics 251 (1995) 215–228

TECTONOPHYSICS

# Mantle structure and seismotectonics of the Sunda and Banda arcs

Nanang T. Puspito [a], Kunihiko Shimazaki [b]

[a] *Department of Geophysics and Meteorology, Bandung Institute of Technology, Jalan Ganesha 10, Bandung 40132, Indonesia*
[b] *Earthquake Research Institute, the University of Tokyo, Yayoi 1-1-1, Bunkyo-ku, Tokyo 113, Japan*

Received 24 March 1994; accepted 1 June 1995

**Abstract**

We have examined the mantle structure and seismotectonic features of the Sunda and Banda arcs, Indonesia, based on the P-wave tomographic images, focal mechanism solutions, gravity anomaly and heat-flow data. On the basis of slab morphology and seismicity, we can divide the arcs into three parts, the Western Sunda, Eastern Sunda, and Banda arc. The slab-like tomographic image penetrates to a depth of about 500 km below the Western Sunda arc where seismicity does not exceed a depth of 250 km. In the Eastern Sunda arc, where a seismic gap exists between 300 and 500 km depths, the slab appears to be continuous and to penetrate into the lower mantle. Beneath the Banda arc, with seismicity down to a depth of about 650 km, the slab dips gently and does not appear to penetrate into the lower mantle. The positive gravity anomaly shows a systematic pattern, namely, the anomaly along the Eastern Sunda arc is larger than that in the Western Sunda and the Banda arcs. Along the back-arc side of the Sunda and Banda arcs, the heat flow decreases from the west to the east. Seismic strain release from the shallow earthquakes calculated from the CMT solutions show the strain axes to be oblique to the structural trends.

The CMT solutions show that the Eastern Sunda arc is characterized by normal earthquakes along the trench and back-arc thrusting earthquakes north of the volcanic line. In the Western Sunda and the Eastern Sunda arcs, earthquakes of the down-dip extension type dominate the slab down to a depth of 200 km while down-dip compression earthquakes occur below 500 km depth. In the Banda arc, deep earthquakes show down-dip extension to a depth of 500 km; below this depth the state of stress is not clearly defined.

## 1. Introduction

Island arcs are among the most interesting tectonic features in the world. These regions are composed of oceanic trenches, non-volcanic and volcanic arcs, and back-arc systems. They have characteristic features in common: recent volcanic activity, deep-sea trenches and deep earthquakes characterize the island arcs (e.g. Sugimura and Uyeda, 1973). However, if we examine those common features in detail, along with other important geophysical data such as gravity anomaly, heat flow, and topography, we are able to recognize that there are dissimilarities among the island arcs. For example, the double-planed deep seismic zone (Hasegawa et al., 1978) is a special feature of the northeastern Japan arc. This feature is not always found beneath island arcs, not even in the other regions of the Japanese islands. Thus, the investigation of dissimilarities of those seismological and geophysical features among the island arcs may improve our understanding of island-arc tectonics. In this study we have chosen the Sunda and Banda arcs of Indonesia as study region. We have attempted to examine the seismological and geophysical data in


*SSDI* 0040-1951(95)00063-1

detail and discuss their possible correlation with problematic tectonic features of the region.

The Sunda and Banda arcs of Indonesia (Fig. 1) provide various modern examples of convergent processes and products that have made the region one of the best sites for seismotectonic studies of island arcs. The arcs are considered as products of the great Burma–Banda subduction system (Hamilton, 1979, 1989), where the convergence of the southeastern block of the Eurasian and Indian–Australian plate is taking place. The Sunda arc, extending westward from Sumba passing along Java and Sumatra to the Andaman Islands, is considered to be an active continental margin or continental arc (Uyeda and Kanamori, 1979). Along the arc, the Indian oceanic plate is being subducted beneath the Eurasian plate. The seismic activity west of the Sunda strait (which separates Sumatra from Java) does not exceed a depth of 250 km. In the east of the strait, the maximum depth reaches about 650 km with a gap of seismicity between 300 and 500 km (Fitch and Molnar, 1970; Newcomb and McCann, 1987). The Banda arc extends eastward from Sumba passing along Tanimbar Islands. In the Banda Sea region, the arc curves sharply counterclockwise to a westward trend in the north through Buru Island. The southern limb of the arc is the place of collision between the northward moving Australian continental plate and the southeasternmost part of the Eurasian plate. Beneath the southern limb of the arc, the seismic zone dips northward to a depth of about 650 km. In the east, the seismic zone curves to define a basin-shaped zone that plunges gently westward (Cardwell and Isacks, 1978).

We divide the Sunda and Banda arcs into three regions based on differences in seismicity and slab morphology (Puspito et al., 1993), i.e. the Western Sunda, Eastern Sunda, and the Banda arcs (Fig. 2 shows the three regions). For each region we present a cross-section of P-wave velocity, earthquake distribution, compression ($P$) and tension ($T$) axes of focal mechanism solution, gravity anomaly, topogra-

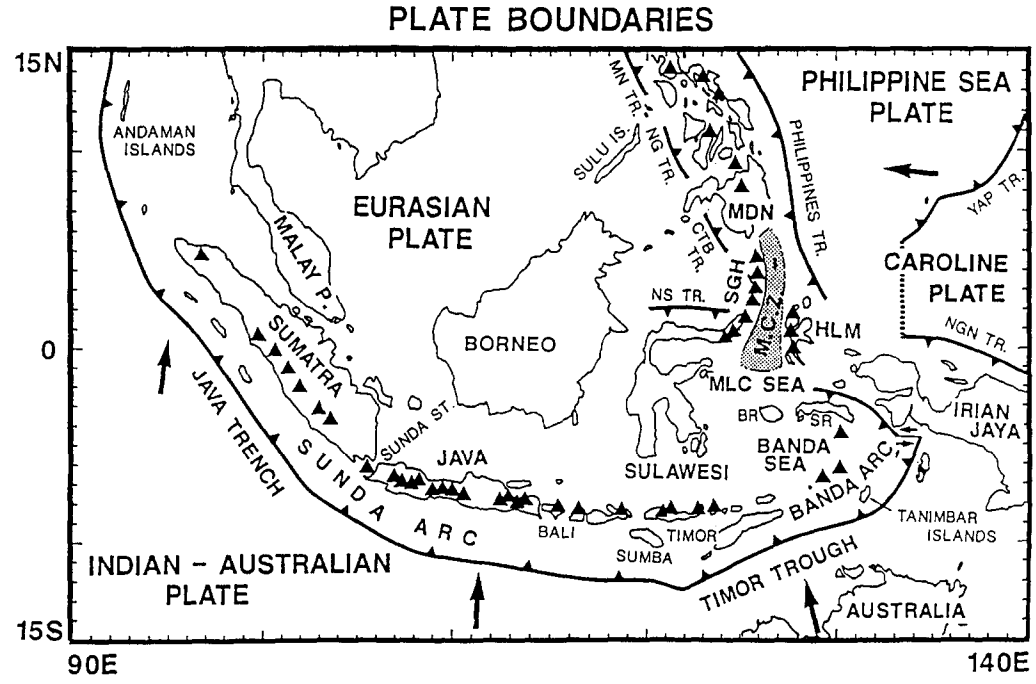


Fig. 1. Tectonic map of the Sunda and Banda arcs, Indonesia. Triangles denote active volcanoes. The large arrows indicate the direction of plate motions relative to the Eurasian plate. *BR* = Buru; *CTB TR* = Cotabato trench; *HLM* = Halmahera arc; *MCZ* = Molucca Collision Zone; *MDN* = Mindanao; *MLC SEA* = Molucca Sea; *MN TR* = Manila trench; *NG TR* = Negros trench; *NGN TR* = New Guinea trench; *NS TR* = North Sulawesi trench; *SGH* = Sangihe arc; *SR* = Seram (adopted from Puspito et al., 1993).

phy, and heat-flow data. The cross-sections are roughly perpendicular to the structural trends (Fig. 2). We have examined the detailed seismotectonic features of the arcs on the basis of these cross-sections. In order to clarify the characteristics of the arcs, we also discuss the tectonic implications.

## 2. Data

We have adopted the three-dimensional P-wave velocity structure from the seismic tomography work of Puspito et al. (1993), who obtained the P-wave tomographic image by using the ARTB (Algebraic Reconstruction Technique of Bayesian type) method originally developed by Hirahara (1988). They employed a dataset of 118,203 P-wave traveltimes of local and teleseismic earthquakes taken from the ISC (International Seismological Center). The P-wave tomographic image is presented in term of the slowness perturbation with respect to the velocity model of Herrin (1968).

We have compiled the focal mechanism solutions from the centroid moment tensor (CMT) solutions obtained by the Harvard group (e.g. Dziewonski and Woodhouse, 1983) and selected the solutions that have small values of non-double couple component (e.g. Kawakatsu, 1991). We have selected the CMT solutions for 321 events that occurred in the period 1977–1991 with magnitudes $Ms \geq 5.0$. In addition to the above data, we have determined the CMT solutions based on the algorithm developed by Kawakatsu (1989) for earthquakes that occurred in 1992, and performed the CMT inversion by utilizing the long-period seismic waveform data taken from IRIS (Incorporated Research Institutions for Seismology). We have determined the CMT solutions for 42 events with magnitudes $Ms \geq 5.0$. Fig. 3 shows the projected compression ($P$) and tension ($T$) axes of the CMT solutions for shallow earthquakes that occurred in the period 1977–1992. Fig. 3 shows that in the Eastern Sunda arc, especially along the trench in the south of Bali, the compression ($P$) axes appear to be parallel to the structural trend while the

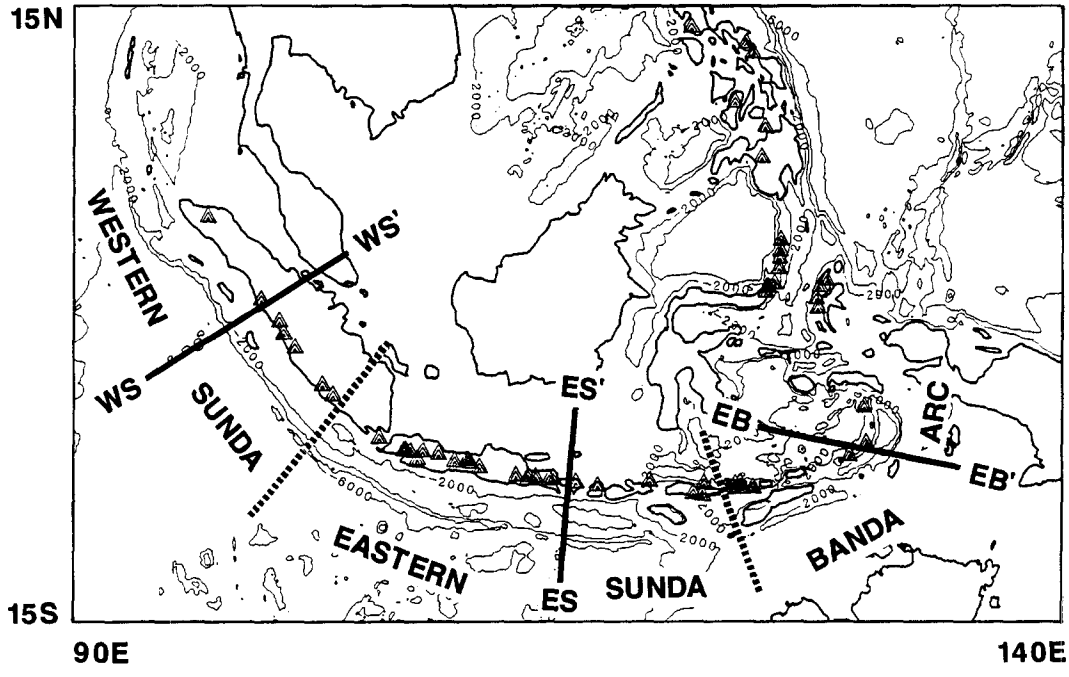


Fig. 2. The three studied regions along the Sunda and Banda arcs of Indonesia, the Western Sunda, Eastern Sunda, and Banda arcs. The division is based on the slab morphology and seismicity. The dotted lines show the proposed boundaries of the three regions. The three solid lines show the cross-sections of Fig. 7. The triangles denote active volcanoes, the contour lines show the bathymetry.

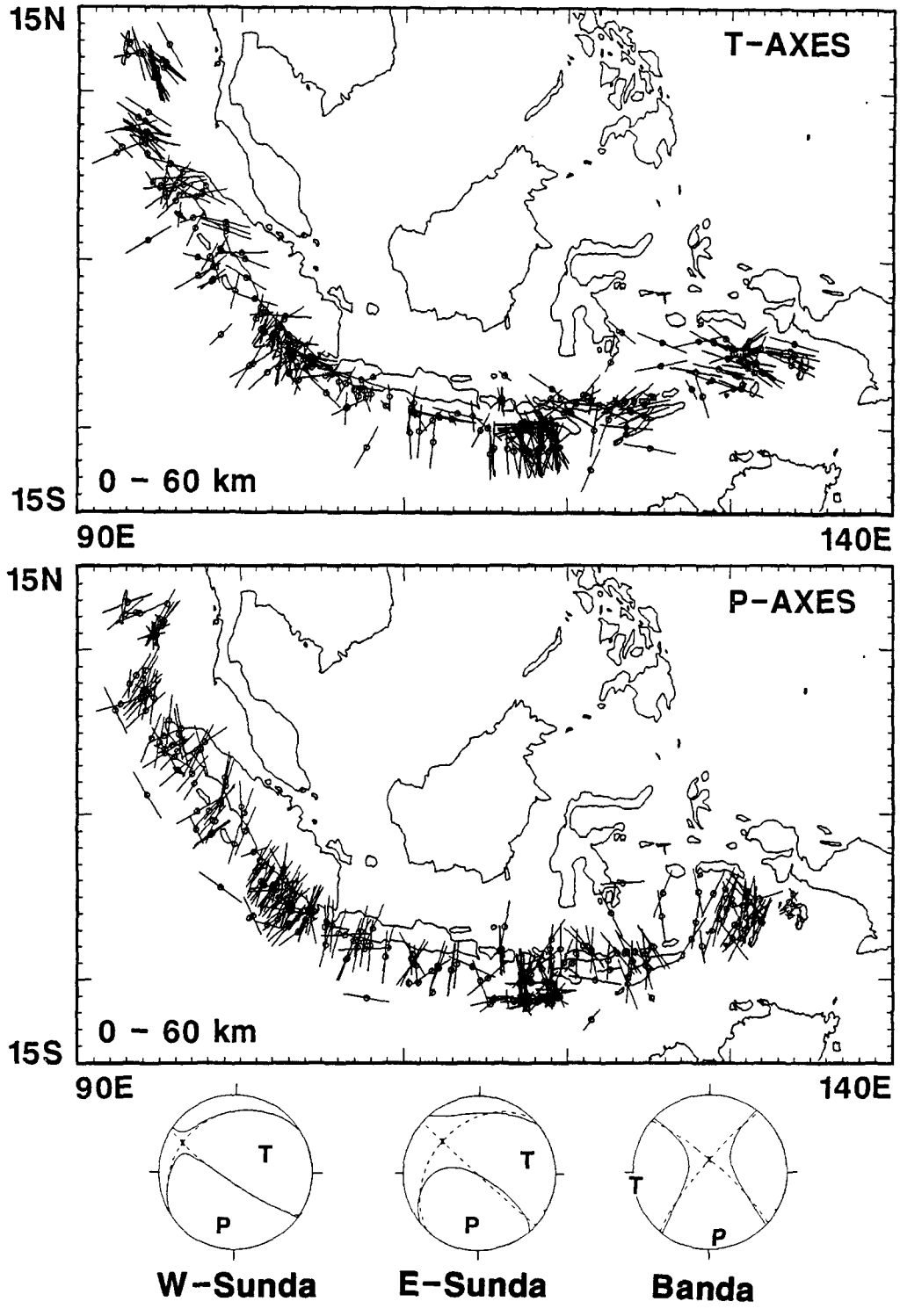
15N
T-AXES
0 – 60 km
15S
90E
140E
15N
P-AXES
0 – 60 km
15S
90E
140E
T
P
W-Sunda
T
P
E-Sunda
T
P
Banda

tension ($T$) axes are perpendicular to this trend. These features represent shallow normal earthquakes within the bending oceanic plate.

In the bottom of Fig. 3 we have also plotted the regional seismic strain of the shallow earthquakes calculated from the CMT solutions for each region. We employed 211 CMT solutions for calculating the regional seismic strain. In this study, the regional seismic strain is an average of all CMT solutions for each region. The calculation is done by averaging all CMT solutions for each region. The regional seismic strain for each region shows that the strain axes are oblique to the structural trends.

We have adopted the regional gravity anomaly data from the work of Haxby et al. (1983). The data consist of the free-air anomaly for the land region and the SEASAT-derived anomaly for the ocean region for every $5' \times 5'$ point. Haxby and his colleagues digitized the free-air anomaly from the published gravity anomaly map. The SEASAT-derived anomaly is derived from the difference between the SEASAT altimeter measured sea surface and the GEM-10B geoid of NASA. Fig. 4 shows the compiled gravity anomaly data. The gravity anomaly data generally show a pattern that is usually found in island-arc regions. A large negative gravity anomaly is found along the trench axis and a large positive gravity anomaly dominates the coastal areas. The positive gravity anomaly (Fig. 4a) shows a systematic pattern, namely, the anomaly along the Eastern Sunda is larger than that in the Western Sunda and Banda arcs.

We have compiled the heat-flow data from several published data (Bowin et al., 1980; Carvalho et al., 1980; Thamrin, 1985; van Gool et al., 1987; Matsubayashi and Nagao, 1991; Nurusman and Subono, 1992). Most of the heat-flow measurements in the Indonesian region have been conducted in the sedimentary basins where oil-industry activities are concentrated (Nurusman and Subono, 1992). Only very few measurements have been carried out in the deep-sea regions. We then averaged the compiled data for a block size of $1° \times 1°$. Fig. 5 shows the averaged heat-flow map. We have presented the data in their numerical values; in addition, possible contours also have been drawn. The most interesting feature of these data is the characteristic heat-flow distribution along the back-arc sides of the Sunda and Banda arcs. Heat-flow values in the Western Sunda arc range from high to very high, in the Eastern Sunda arc they range from moderate to high, and in the Banda arc from low to moderate values. These features are clearly seen if we plot the original data only along the back-arc sides of the arcs. Fig. 6 shows the original heat-flow data taken along the back-arc sides of the arcs plotted against the longitude of the data location. The plotted data clearly show the heat flow decreasing from the west to the east along the back-arc sides of the Sunda and Banda arcs.

## 3. Features of the cross-sections

We present cross-sections of seismological and geophysical features for each region along the Sunda and Banda arcs in order to examine the variations in the seismological and geophysical characteristics along the arcs. Fig. 2 shows the cross-section lines. We have plotted all the compiled data, gravity anomaly, heat flow, focal mechanism solution, and the P-wave velocity structure. We have also plotted the calculated gravity anomaly caused by the deep slab. We only calculated the effect of slab below 100 km depth. We approximate the geometry of the deep slab based on the simplified form of the slab-like tomographic features and the distribution of earthquakes. For calculation of the gravity anomaly caused by the deep slab, we assumed a two-dimensional slab. The slab and the mantle both are assumed to be homogeneous bodies. We assumed that the density contrast is 0.06 g/cm between the cold descending slab and its surrounding mantle. This simple calculation is based on the two-dimensional method of Talwani et al. (1959). For the heat-flow data, we have not plotted the averaged values; instead, we

Fig. 3. The projected tension ($T$) and compression ($P$) axes of the CMT solutions for the shallow events that occurred in the period 1977–1992. The regional seismic strain of the shallow events calculated from the CMT solutions for each region is given in the lower part of the figure.

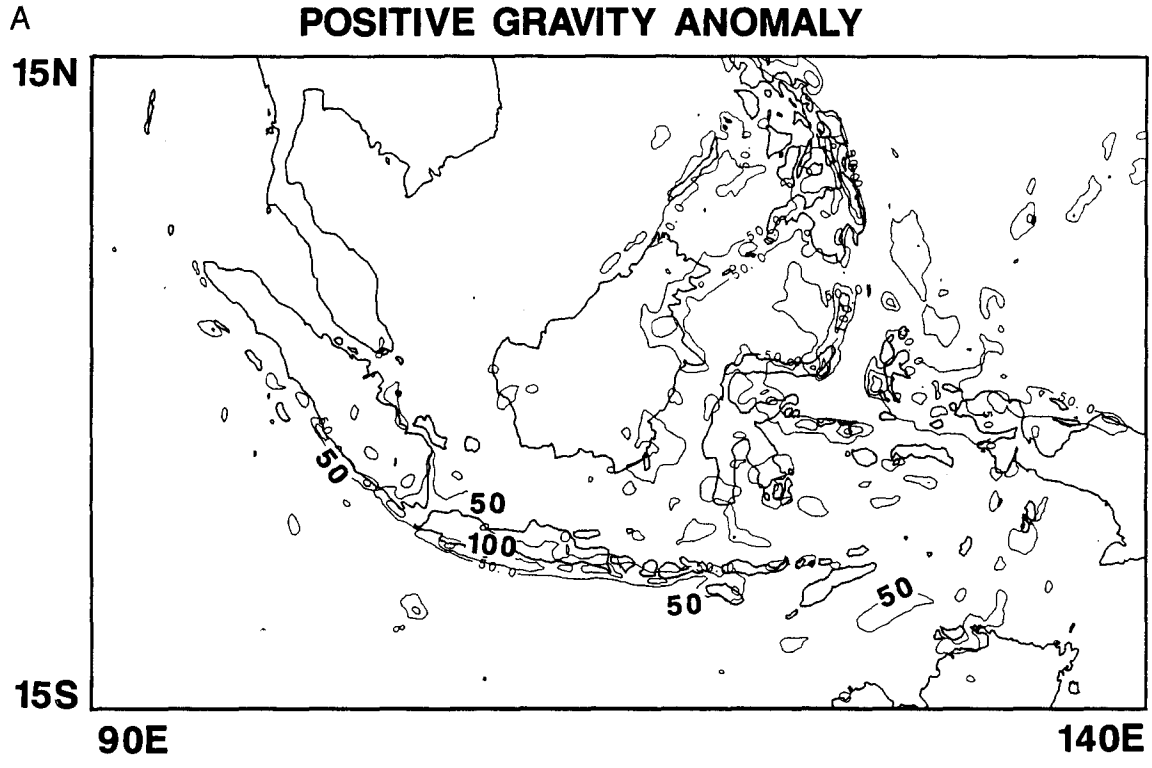
A
POSITIVE GRAVITY ANOMALY
15N
15S
90E
140E
50
50
100
50
50

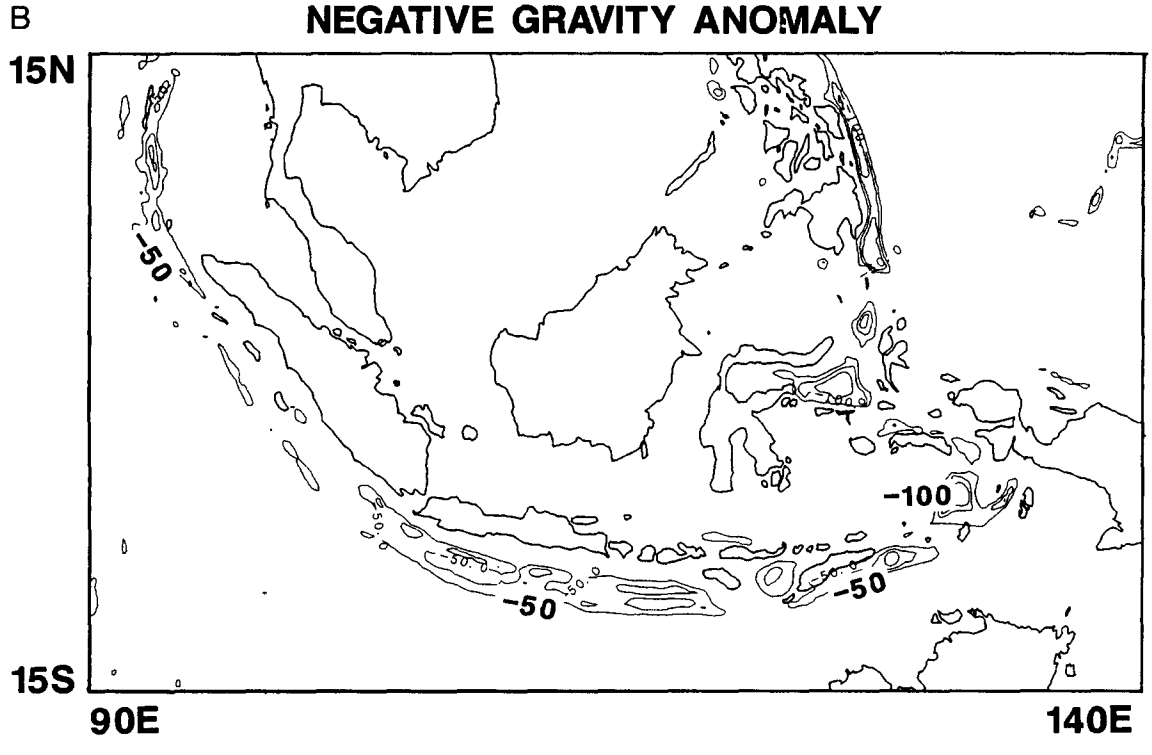
B
NEGATIVE GRAVITY ANOMALY
15N
15S
90E
140E
-50
-100
-50
-50

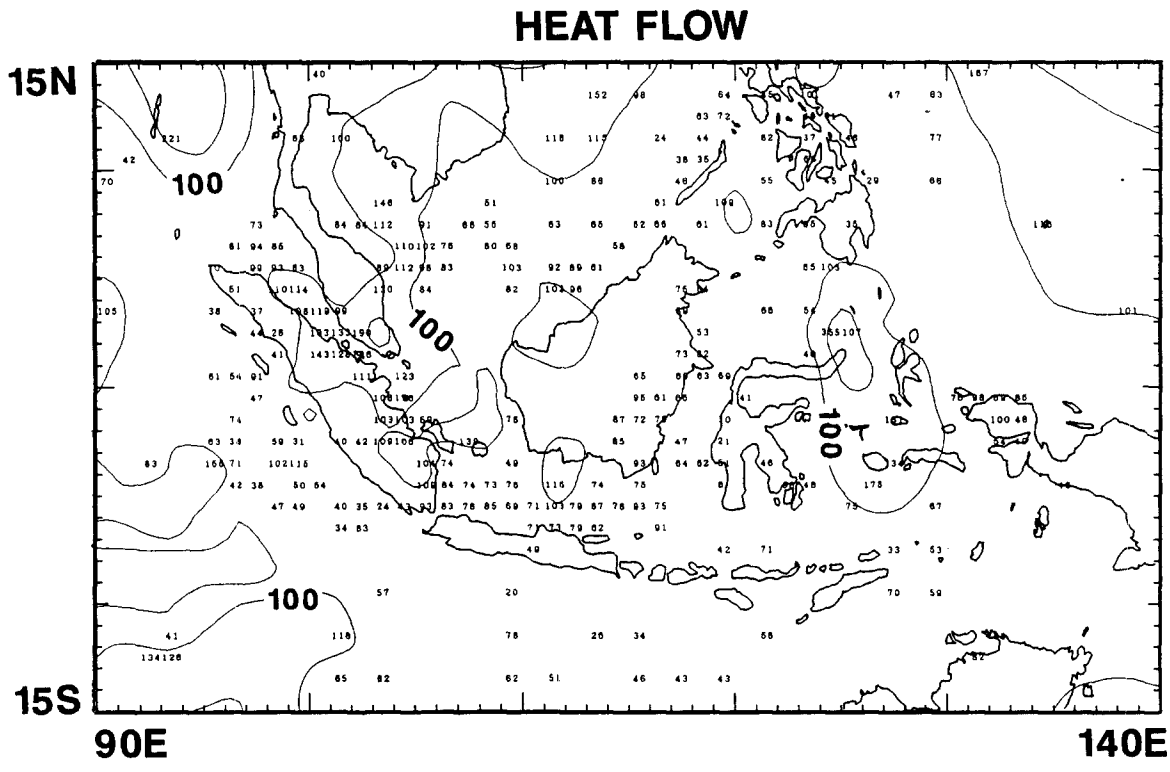


Fig. 5. The averaged heat-flow map. The original data are averaged for each 1° × 1° block. Heat-flow values are in mW/m$^2$. The possible contour lines are also shown.

present the original data. The earthquakes focal mechanism solutions are represented by their projected compression ($P$) and tension ($T$) axes. The P-wave velocity structure is presented in terms of the slowness perturbation with respect to the Herrin velocity model (Puspito et al., 1993). In these cross-sections we have also plotted the topography, active and Quaternary volcanoes, and the well-located hypocenters of earthquakes whose focal depth is constrained by pP–P taken from the ISC Bulletins. The cross-section widths are 0.5° for the gravity anomaly and topography data, 2° for the heat-flow data, and 1° for the seismicity and the compression ($P$) and tension ($T$) axes. The cross-sectional features are shown in Fig. 7, (a) for the Western Sunda arc, (b) for the Eastern Sunda arc, and (c) for the Banda arc. The main features will be described below.

### 3.1. The Western Sunda arc

The *WS–WS'* cross-section (Fig. 7a) passes through the Java trench, Sumatra, and the Malay Peninsula (Fig. 2). The gravity anomaly shows a typical pattern observed in most island-arc regions. A large negative anomaly (about −60 mgal) is found in the trench axis; a large positive anomaly (about 70 mgal) is found near the coast line. The calculated gravity anomaly caused by the deep slab shows a peak of about 170 mgal near the volcanic front. The abundant heat-flow data, mainly provided by oil industries in Sumatra, shows that the heat flow

Fig. 4. The gravity anomaly map. The upper part (a) shows the positive gravity anomaly and the lower part (b) shows the negative gravity anomaly. The contours are in mgal. The data are taken from the work of Haxby et al. (1983).

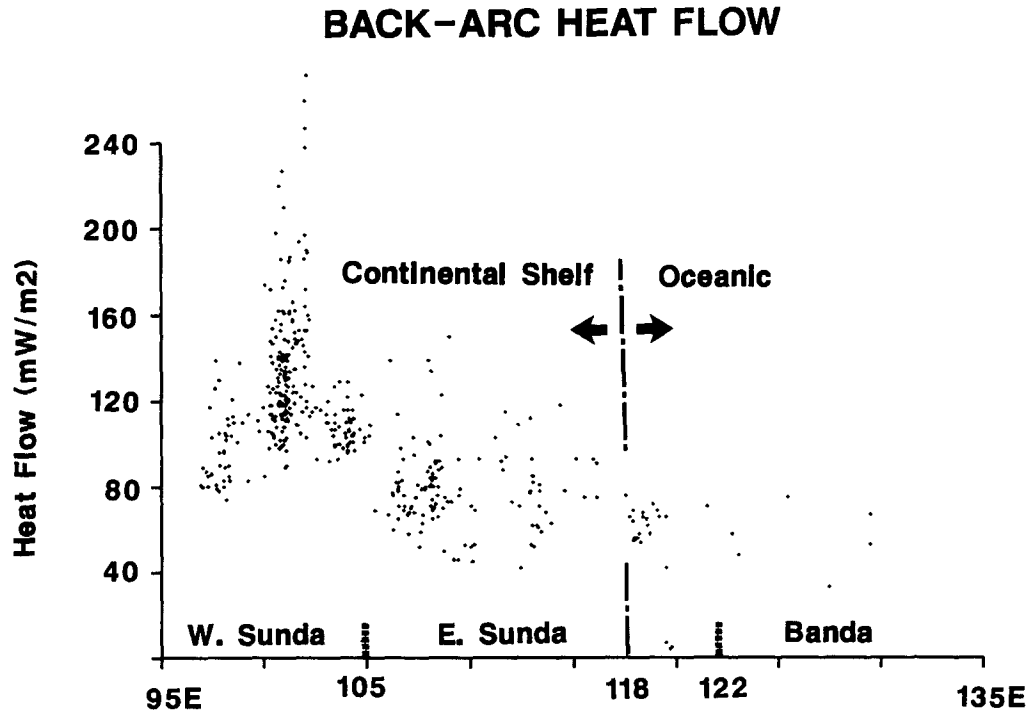


Fig. 6. The heat flow along the back-arc side. The original data are taken along the back-arc side of the Sunda and Banda arcs. The horizontal axis shows the longitude of the original data. The dotted lines shows the proposed boundaries between the Western Sunda, Eastern Sunda, and Banda arcs.

in the back-arc region ranges from high to extremely high, mostly higher than 80 mW/m. In the ocean region, the heat flow varies from low to high. The dip of the seismic zone that does not exceed 250 km depth below Sumatra is about 30°. The obtained P-wave tomographic image shows that the descending slab is well delineated by the slab-like high-velocity zone. The slab-like high-velocity zone agrees well with the distribution of earthquakes. The slab appears to penetrate down to a depth of 500 km, suggesting the existence of aseismic slab below Sumatra. The focal mechanism data indicate that the deep earthquakes are dominated by the down-dip tension type. The shallow strike-slip earthquakes near the volcanic front represent the shallow seismicity associated with the right-lateral Sumatra fault.

### 3.2. *The Eastern Sunda arc*

The *ES–ES'* cross-section (Fig. 7b) passes through the Java trench, Bali to the south of Borneo (Fig. 2). The topography profile clearly shows large topographic features in the oceanic region and the corresponding variations are found in the gravity anomaly profile. Two peaks of large negative gravity anomaly are found. One (about −100 mgal) is located along the trench axis and the other one (about −80 mgal) characterizes the fore-arc basin. Large positive gravity anomaly (reaches about 130 mgal) is found near the coast line where the calculated gravity anomaly caused by deep slab reaches about 200 mgal. The heat flow in the back-arc basin is moderate (about 80 mW/m) while in the ocean region it is low. The seismic zone in this cross-section extends down to a depth of about 650 km but a seismic gap exists in the depth range 300–500 km. The descending slab is clearly delineated by the slab-like high-velocity zone. The slab-like high-velocity zone can be traced down to the lower mantle. The earthquake focal mechanism solutions indicate down-dip tension type for the intermediate-depth earthquakes, while the deep earthquakes are dominated by down-dip compression

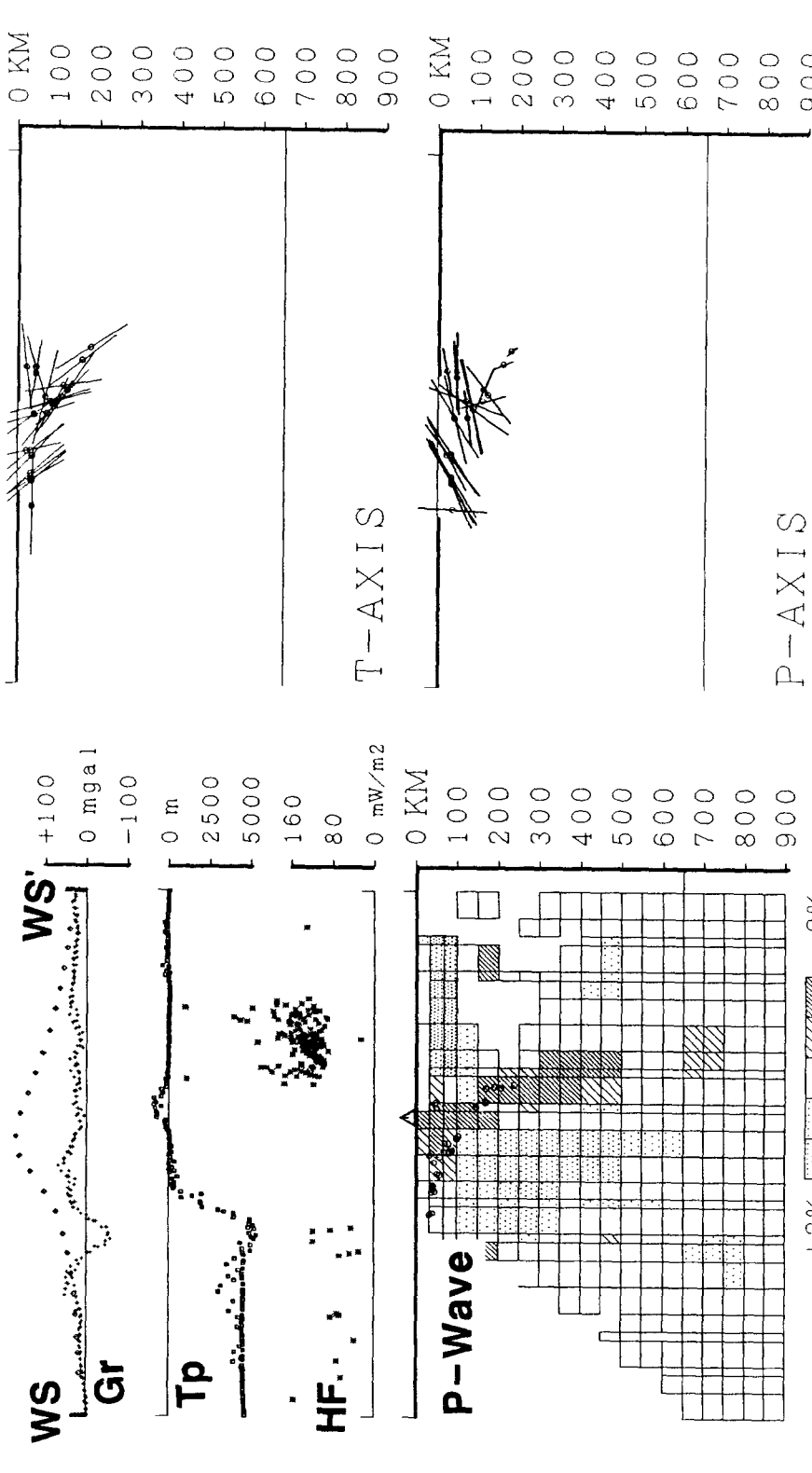


Fig. 7. Cross-sectional features along the Sunda and Banda arcs, (a) for the Western Sunda, (b) for the Eastern Sunda, and (c) for the Banda arcs. Cross-section lines are shown in Fig. 2. On the left from top to bottom are: gravity anomaly (*Gr*), topography (*Tp*), heat flow (*HF*), and the P-wave velocity structure (*P-Wave*). In the gravity anomaly, the diamonds denote the calculated gravity anomaly caused by deep slab and the pluses denote the compiled gravity anomaly data. In the P-wave velocity structure, triangles denote active and Quaternary volcanoes and the circles denote the well-located earthquake hypocenters taken from ISC. The P-wave velocity is presented in term of slowness perturbations with minus denoting high velocity and plus denoting low velocity. The right side shows the projected tension (*T*) and compression (*P*) axes of the CMT solutions.

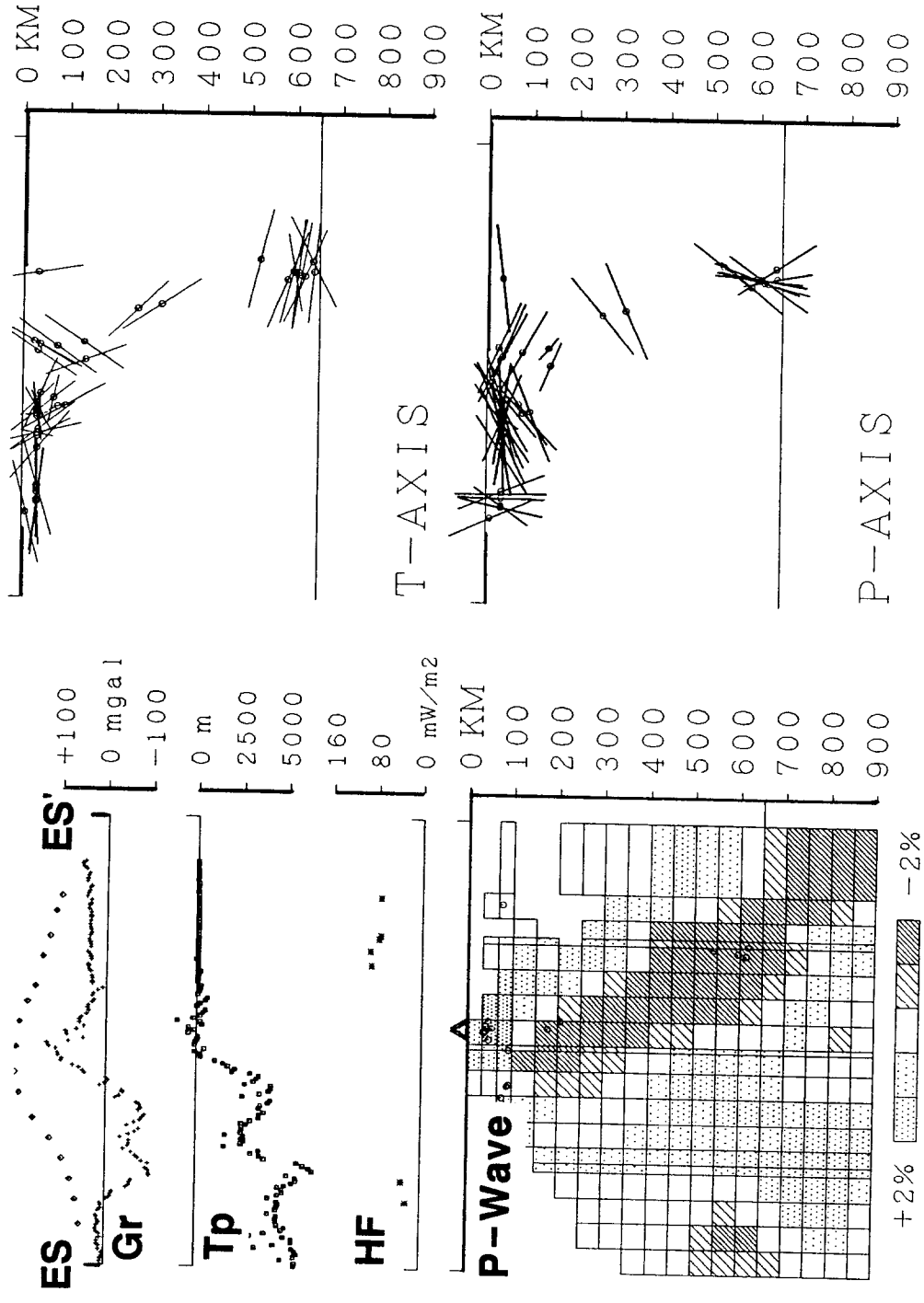


Fig. 7 (continued).

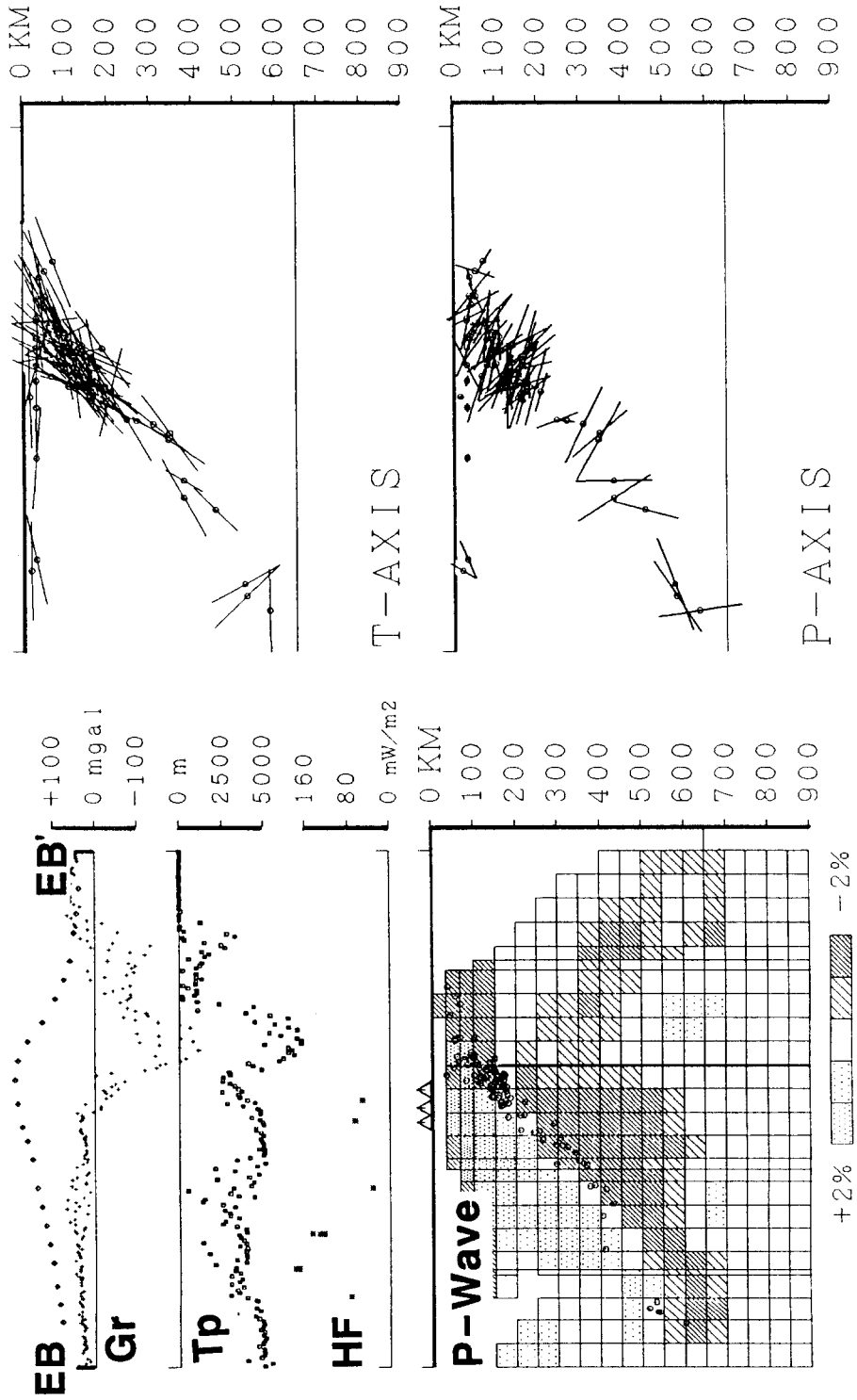


Fig. 7 (continued).

type. Shallow earthquakes near the trench axis are clearly dominated by normal earthquakes type. These shallow normal earthquakes can be also found along the trench in the east of this cross-section. Among them is the 1977 Sumba earthquake ($Ms = 7.9$). The area north of the volcanic front is characterized by the shallow thrust earthquakes which indicate back-arc thrusting in this region. This kind of thrust earthquakes can be found also in the east of this cross-section. Among them is the 1992 Flores earthquake ($Ms = 7.5$).

### 3.3. The Banda arc

The *EB–EB′* cross-section (Fig. 7c) represents the eastern part of the Banda arc (Fig. 2). The cross-section is taken across the Timor trough and the entire Banda Sea including the outer- and inner-arcs and the Weber deep. This cross-section cuts across the most complicated pattern of submarine topography, especially large topographic features in the Banda Sea region. The water depth in the Weber deep reaches about 8000 m and is much deeper than the Timor trough. The Weber deep is characterized by a very large negative gravity anomaly (about −250 mgal) while the Timor trough is characterized by a large negative anomaly of about −120 mgal. The calculated effect of deep slab shows its maximum (about 190 mgal) near the volcanic front. The gravity anomaly in the back-arc region shows a positive anomaly without conspicuous peak. Heat flow in the back-arc region varies from low to high. The dip of the Wadati-Benioff zone is about 45° to a depth of about 650 km. The slab-like high-velocity zone agrees fairly well with the distribution of earthquakes. The slab does not appear to penetrate into the lower mantle. The focal mechanism data clearly show that the deep earthquakes down to about 500 km depth are of the down-dip tension type. Below this depth the state of stress is not clearly defined. Shallow earthquakes in the back-arc region are characterized by the strike-slip earthquake type.

## 4. Discussion and conclusions

The regional gravity anomaly (Figs. 4 and 7) generally depicts a pattern that is commonly observed in island arcs, a large negative anomaly along the trench axis and a large positive anomaly along the arc line. However, if we look at the data in more detail, we recognize that they show certain characteristics along the Sunda and Banda arcs. The regional positive gravity anomaly shows a systematic pattern, the positive gravity anomaly in the Eastern Sunda being larger than that in the Western Sunda and Banda arcs. First we suspect that this significant variation is partly caused by the effect of a deep slab. However, our simple calculation of the gravity anomaly caused by the deep slab has failed to explain this significant variation in the short-wavelength gravity anomaly. The peak of the calculated gravity anomaly caused by the deep slab does not fit with the peak of the positive gravity anomaly that is found along the coast line (Fig. 7). This discrepancy might be caused by the shallow structural effects, such as variation in crustal thickness and the existence of mineral bodies in the crust. However, detailed study is needed to clarify this point.

The averaged heat-flow map (Fig. 5) and the cross-sections (Fig. 7) generally show a pattern which is commonly observed across subduction regions, low near the trench axis and its ocean region and moderate to high in the arc and its back-arc side. Along the back-arc side of the Sunda and Banda arcs (Figs. 5 and 6), the heat flow generally decreases from west to east. Heat flow in the back-arc side of the Western Sunda arc is higher than that in the Eastern Sunda and the Banda arcs. A sharp decline of heat-flow values can be seen around the 118°E line (Fig. 6). The line separates the continental and oceanic crustal types beneath the back-arc side of the Sunda and Banda arcs (Katili, 1975; Hamilton, 1979). This variation may be caused by variation in crustal thickness along the back-arc side of the arcs. Unfortunately, there is very few detailed information on the crustal thickness along the back-arc side of the arcs. Thus, it is difficult to correlate the crustal thickness with the heat-flow distribution along the back-arc side of the arcs.

The P-wave tomographic image (Fig. 7a) shows that the slab penetrates to a depth of about 500 km below the Western Sunda arc where the seismicity does not exceed a depth of 250 km. In the Eastern Sunda arc where a seismic gap exists between depths of 300 and 500 km, the slab appears to be continuous

and to penetrate into the lower mantle (Fig. 7b). The variation in the depth of slab penetration along the Western and Eastern Sunda may also be explained as being due to the effects of oblique subduction in the Western Sunda arc. The tectonic meaning of the existence of aseismic slab in the subduction zones, as the case in the Western Sunda and the Eastern Sunda arcs, still remains unclear. A similar case is found in the Tonga region where the slab seems to be continuous in the depth range where a seismic gap exists (Taniyama et al., 1990). For the penetration of slab into the lower mantle, one possible explanation would be the concept of whole mantle convection. However, this topic is still in dispute. In the Banda arc, where seismicity continues down to a depth of about 650 km, the slab dips gently and does not appear to penetrate into the lower mantle (Fig. 7c), which is different in the Eastern Sunda arc. The curving of the slab and the gentle dip (Cardwell and Isacks, 1978; Puspito et al., 1993) may prevent the slab to penetrate into the lower mantle. The shallow part of the Banda slab is the Australian continental lithosphere while the deeper part is the Indian oceanic lithosphere (Hamilton, 1979). Since the density of the Australian continental lithosphere is supposed to be less than that of the Banda Sea oceanic lithosphere, the subduction may gradually cease. The incapability of the Banda slab to penetrate into the lower mantle may be due to the gradual decay of subduction of the Australian continental lithosphere.

## Acknowledgements

We thank Profs. T. Seno, T. Miyatake and H. Kawakatsu and Dr. Y. Yamanaka of the Earthquake Research Institute of the University of Tokyo, for discussion.

## References

Bowin, C.O., Purdy, G.M., Johnston, C., Shor, G.G., Lawver, L., Hartono, H.M.S. and Pezek, J., 1980. Arc–continent collision in Banda Sea region. Am. Assoc. Pet. Geol. Bull., 64: 868–915.

yardwell, R. and Isacks, B., 1978. Geometry of the subducted lithosphere beneath the Banda Sea in eastern Indonesia from seismicity and fault plane solutions. J. Geophys. Res., 83: 2825–2853.

Carvalho, H. da S., Purwoko, Siswoyo, Thamrin, M. and Vacquier, V., 1980. Terrestrial heat flow in the tertiary basin of central Sumatra. Tectonophysics, 69: 163–188.

Dziewonski, A.M. and Woodhouse, J.H., 1983. An experiment in systematic study of global seismicity: centroid-moment tensor solutions for 201 moderate and large earthquakes in 1981. J. Geophys. Res., 75: 1431–1444.

Fitch, T.J. and Molnar, P., 1970. Focal mechanism along inclined earthquake zones in Indonesia–Philippine region. J. Geophys. Res., 75: 1431–1444.

Hamilton, W., 1979. Tectonics of the Indonesian Region. US Geol. Surv. Prof. Pap., 1078, 345 pp.

Hamilton, W., 1989. Convergent-plate tectonics viewed from the Indonesian region. In: A. Sudradjat, H.D. Tjia, S. Asikin and A.N. Katili (Editors), J.A. Katili Commemorative Volume. Geol. Indones., Indones. Assoc. Geol., pp. 35–88.

Hasegawa, A., Umino, N. and Takagi, A., 1978. Double-planed structure of the deep seismic zone in the northeastern Japan arc. Tectonophysics, 101: 245–265.

Haxby, W.F., Karner, G.D., LaBrecque, J.L. and Weissel, J.K., 1983. Digital images of combined oceanic and continental data sets and their use in tectonic studies. EOS Trans. Am. Geophys. Union, 64: 995–1004.

Herrin, E., 1968. Seismological tables for P phases. Bull. Seismol. Soc. Am., 58: 1193–1241.

Hirahara, K., 1988. Detection of three-dimensional velocity anisotropy. Phys. Earth. Planet. Inter., 51: 71–85.

Katili, J.A., 1975. Volcanism and plate tectonics in the Indonesian island arcs. Tectonophysics, 26: 165–188.

Kawakatsu, H., 1989. Centroid single force inversion of seismic waves generated by landslides. J. Geophys. Res., 94: 12, 363–12, 374.

Kawakatsu, H., 1991. Enigma of earthquakes at ridge–transform–fault plate boundaries: distribution of non-double couple parameter of harvard CMT solutions. Geophys. Res. Lett., 18: 1103–1106.

Matsubayashi, O. and Nagao, T., 1991. Compilation of heat flow data in southeast asia and its marginal seas. In: V. Čermák and L. Rybach (Editors), Terrestrial Heat Flow and the Lithosphere Structure. Springer, Heidelberg, pp. 444–456.

Newcomb, K.R. and McCann, W.R., 1987. Seismic history and seismotectonics of the Sunda arc region. J. Geophys. Res., 92: 421–439.

Nurusman, S. and Subono, S., 1992. Heat Flow Measurements in Indonesia. Pertamina, Jakarta (unpubl. rep.).

Puspito, N.T., Yamanaka, Y., Miyatake, T., Shimazaki, K. and Hirahara, K., 1993. Three-dimensional P-wave velocity structure beneath the Indonesian region. Tectonophysics, 220: 175–192.

Sugimura, A. and Uyeda, S., 1973. Island Arcs: Japan and its Environs. Elsevier, Amsterdam.

Talwani, M., Worzel, J.L. and Landisman, M., 1959. Rapid gravity computations for two-dimensional bodies with application to the Mendocino submarine fracture zone. J. Geophys. Res., 64: 49–59.

Taniyama, H., Shimazaki, K. and Hiarahara, K., 1990. Corrections for receiver structure in teleseismic travel time inversion: 3-D

P-wave velocity structure of the New Hebrides. EOS Trans. Am. Geophys. Union, 71: 897.

Thamrin, M., 1985. An investigation of the relationship between the geology of Indonesian sedimentary basins and heat flow density. Tectonophysics, 121: 45–62.

Uyeda, S. and Kanamori, H., 1979. Back-arc opening and the mode of subduction. J. Geophys. Res., 84: 1049–1061.

Van Gool, M., Huson, W.J., Prawirasasra, R. and Owen, T.R., 1987. Heat flow and seismic observations in the northwestern Banda Arc. J. Geophys. Res., 92: 2581–2586.